Molecular Pharmacology Fast Forward. Published on August 5, 2011 as DOI: 10.1124/mol.111.073205
This article has not been copyedited and formatted. The final version may differ from this version.

MOL #73205

TTA-P2 is a potent and selective blocker of T-type calcium channels in rat sensory neurons and a novel antinociceptive agent

WonJoo Choe, Richard B. Messinger, Emily Leach, Veit-Simon Eckle, Aleksandar Obradovic, Reza Salajegheh, Vesna Jevtovic-Todorovic and Slobodan M. Todorovic

Dept. of Anesthesiology (RBM, EL, AO, RS, VJT, SMT), Neuroscience (VJT, SMT), Neuroscience Graduate Program (SMT, VJT) at the University of Virginia Health System, Charlottesville, VA;
Dept. of Anesthesiology, InJe University Ilsan Paik Hospital & College of Medicine, Seoul, Korea (WJC);
Department of Anesthesiology and Intensive Care Medicine, Tuebingen University Hospital, Eberhard-Karls University, Tuebingen, Germany (V-SE)

Molecular Pharmacology Fast Forward. Published on August 5, 2011 as DOI: 10.1124/mol.111.073205
This article has not been copyedited and formatted. The final version may differ from this version.

RUNNING TITLE PAGE

Running title: TTA-P2 blocks T-currents in the rat sensory neurons

Corresponding Author: Slobodan M. Todorovic
Department of Anesthesiology, University of Virginia Health System, Mail Box 800710, Charlottesville, VA 22908-0710
Phone 434-924-2283, Fax 434-982-0019, Email:st9d@virginia.edu

Number of figures: 7
Number of tables: 0
Number of text pages: 34
Number of words in Abstract: 234
Number of words in Introduction: 735
Number of words in Discussion: 1187

Abbreviations:

DRG (dorsal root ganglion)
LVA (low-voltage-activated)
TEA-OH (tetraethylammonium hydroxide)
HEK (human embryonic kidney)
PWL (paw withdrawal latency)
STZ (streptozocin)
TMA-OH (tetramethylammonium hydroxide)
TTX (tetrodotoxin)
TTA-P2 (3,5-dichloro-N-[1-(2,2-dimethyl-tetrahydro-pyran-4-ylmethyl)-4-fluoro-piperidin-4-ylmethyl]-benzamide)
PDN (peripheral diabetic neuropathy)
DMSO (dimethylsulfoxide)
BAPTA (1,2-bis(o-aminophenoxy)ethane-N,N,N',N'-tetraacetic acid)
EGTA (ethylene glycol tetraacetic acid)
GTP (guanosine three phosphate)
ECN [(3β, 5α, 17β)-17-hydroxyestrane-3-carbonitrile]
3βOH [(3β, 5β, 17β)-3-hydroxyandrostane-17-carbonitrile]

Molecular Pharmacology Fast Forward. Published on August 5, 2011 as DOI: 10.1124/mol.111.073205
This article has not been copyedited and formatted. The final version may differ from this version.

ABSTRACT

Several agents that are preferential T-type calcium (T-channel) blockers have shown promise as being effective in alleviating acute and chronic pain, suggesting an urgent need to identify even more selective and potent T-channel antagonists. We used small, acutely dissociated dorsal root ganglion (DRG) cells of adult rats to study the *in vitro* effects of 3,5-dichloro-N-[1-(2,2-dimethyl-tetrahydro-pyran-4-ylmethyl)-4-fluoro-piperidin-4-ylmethyl]-benzamide (TTA-P2), a derivative of 4-aminomethyl-4-fluoropiperdine, on T-currents, as well as other currents known to modulate pain transmission. We found that TTA-P2 potently and reversibly blocked DRG T-currents with an IC_{50} of 100 nM and stabilized channel in the inactive state, while high-voltage-activated (HVA) calcium and sodium currents were 100-1,000-fold less sensitive to channel blocking effects. In *in-vivo* studies, we found that intraperitoneal (i.p.) injections of 5 or 7.5 mg/kg of TTA-P2 reduced pain responses in mice in phases 1 and 2 of the formalin test. Furthermore, TTA-P2, at 10 mg/kg i.p., selectively and completely reversed thermal hyperalgesia in diabetic rats treated with streptozocin, but had no effect on the nociceptive response of healthy animals. The anti-hyperalgesic effects of TTA-P2 in diabetic rats were completely abolished by administration of oligonucleotide antisense for $Ca_V3.2$ isoform of T-channels. Thus, TTA-P2 is not only the most potent and selective blocker of T-channels in sensory neurons yet described, but also demonstrates the potential for the pharmacological effectiveness of this approach in addressing altered nociceptive responses in animal models of both inflammatory and neuropathic pain.

Molecular Pharmacology Fast Forward. Published on August 5, 2011 as DOI: 10.1124/mol.111.073205
This article has not been copyedited and formatted. The final version may differ from this version.

INTRODUCTION

Based on the membrane potential at which they gate ion currents, voltage-gated calcium channels are classified as high-voltage activated (HVA) or sustained currents and low-voltage activated (LVA) or transient currents (T-type) (Perez-Reyes, 2003). Different subtypes of HVA currents in the central nervous system are important in regulating fast synaptic transmission. In contrast, neuronal T-channels have key functions in neuronal membrane oscillations and in lowering the threshold for action potential firing in both the peripheral and central nervous systems. Based on cloned sequences of the pore-forming α1 subunit, at least three isoforms of T-channels exist: $Ca_V3.1$ (α1G) (Perez-Reyes et al., 1998), $Ca_V3.2$ (α1H) (Cribbs et al., 1998), and $Ca_V3.3$ (α1I) (Lee et al., 1999). Recent electrophysiological, genetic, molecular, and behavioral studies have suggested that T-channels are crucial in controlling the excitability of sensory neurons, act as signal amplifiers, and make a previously unrecognized contribution to both peripheral and central pain processing (Choi et al., 2007; Todorovic et al., 2001; Jevtovic-Todorovic and Todorovic, 2006; Snutch and David, 2006). Furthermore, *in vivo* experiments showed that use of subtype-specific antisense for knockdown of $Ca_V3.2$ channels in DRG cells completely reversed hyperalgesia in animal models of mechanical injury to the sciatic nerve (Bourinet et al., 2005) and painful diabetic neuropathy (Messinger et al., 2009). This creates interest in further developing pharmacological tools for studies of the function of T-channels in pain pathways and for clinical development of specific pain therapies targeting ion channels in sensory neurons.

While there are many natural toxins or venom components that could be used to study the multiple HVA currents, only recently have substances been identified that are more useful blockers of T-currents. Consistent with this, systemic injections of mibefradil,

Molecular Pharmacology Fast Forward. Published on August 5, 2011 as DOI: 10.1124/mol.111.073205
This article has not been copyedited and formatted. The final version may differ from this version.

a peripherally acting pan-T-channel blocker (Clozel et al., 1997), suppressed cutaneous, thermal, and mechanical nociception in healthy rats (Todorovic et al., 2002), as well as visceral nociception in healthy mice (Kim et al., 2003). Furthermore, the reversal of symptoms of neuropathic pain associated with chronic constrictive injury (CCI) of the sciatic nerve has been demonstrated by systemic and local intraplantar injections of mibefradil (Dogrul et al., 2003). Some clinically used antiepileptics such as phenytoin and ethosuximide are *in vitro* blockers of T-channels in sensory neurons (Todorovic and Lingle, 1998) and potent analgesics when injected into peripheral receptive fields of whole animals (Todorovic et al., 2003). Importantly, some other clinically used analgesic drugs target voltage-gated calcium channels. For example, voltage-gated calcium channels are considered a major cellular target for the anticonvulsant gabapentin and pregabalin, which can relieve diabetes-induced neuropathic pain in some populations of patients (Rogawski and Loscher, 2004). However, the use of gabapentin and related drugs is associated with side effects such as excessive sedation in many patients, which necessitates the search for other novel therapies (Edwards et al., 2008).

The usefulness of mibefradil, a prototypical T-channel blocker, has been questioned since recent studies have demonstrated that this molecule, in addition to affecting T-channels, can affect several other ion channels, including voltage-gated sodium channels in sensory neurons, with a similar potency (Coste et al., 2007). Similarly, the antiepileptic ethosuximide, another representative T-channel blocker and analgesic in animal pain models (Todorovic et al., 2003), affects T-channels and sodium channels in neurons of the central nervous system (CNS) with similar potency (Leresche et al., 1998). This raises the question of whether the analgesic effects of these drugs in behavioral pain paradigms can be attributed only to the antagonism of T-channels. Thus, in spite of the progress made in recent years, pharmacological tools for the study of T-currents are still very limited (see reviews by McGivern, 2006 and Lory and Chemin,

Molecular Pharmacology Fast Forward. Published on August 5, 2011 as DOI: 10.1124/mol.111.073205
This article has not been copyedited and formatted. The final version may differ from this version.

2007), precluding any clinical studies aimed at establishing the potential value of T-channel blockers in treating various pain disorders.

The recent discovery of novel selective T-channel antagonists such as 4-aminomethyl-4-fluoropiperdine is promising because these agents completely block recombinant T-current isoforms with high potency (IC_{50}s 20-100 nM) (Shipe et al., 2008). However, the selectivity, potency, and mechanisms of action of these novel blockers in native cells in pain pathways have not, as yet, been systematically examined. Thus, we hypothesized that one such compound, 3,5-dichloro-N-[1-(2,2-dimethyl-tetrahydro-pyran-4-ylmethyl)-4-fluoro-piperidin-4-ylmethyl]-benzamide (TTA-P2, see Figure 1), may be a potent blocker of native T-currents in rat sensory neurons and, accordingly, a useful tool for studies of the role of T-channels in pain signaling. To test this hypothesis, we have done biophysical studies using patch-clamp experiments with acutely dissociated sensory neurons of rat dorsal root ganglia (DRG) and whole-animal behavioral pain experiments with adult rats and mice.

Materials and Methods

I. *Electrophysiological in vitro studies:* Before the harvest of tissues, rats were deeply anesthetized with isoflurane and rapidly decapitated. For one experiment, we dissected 6-8 lumbar DRGs from both sides of rats. We prepared acutely dissociated DRG cells and used them within 6-8 h for whole-cell recordings as previously described (Todorovic et al., 1998, Nelson et al., 2005, 2007). We focused on small cells (i.e., those with an average soma diameter of 20-30 μm), since functional studies have indicated that most of them are likely polymodal nociceptors belonging to unmyelinated C-type sensory fibers that are capable of responding to noxious mechanical, chemical, and thermal stimuli *in vivo* (McCleskey and Gold, 1999; Campbell and Mayer, 2006). Our previous studies have confirmed that the majority of acutely dissociated small DRG cells express

Molecular Pharmacology Fast Forward. Published on August 5, 2011 as DOI: 10.1124/mol.111.073205
This article has not been copyedited and formatted. The final version may differ from this version.

T-currents that are important for control of membrane excitability (Todorovic et al., 1998, Nelson et al., 2005; 2007).

Recordings were made using standard whole-cell techniques. Series resistance (R_s) and capacitance (C_m) values were taken directly from readings of the amplifier after electronic subtraction of the capacitive transients. Series resistance was compensated to the maximum extent possible (usually ~60%-80%). In most experiments, we used a P/5 protocol for online leak subtractions. The percent reductions in peak current at various concentrations of TTA-P2 were used to generate a concentration-response curve. Mean values were fit to the following Hill function:

$$PB([TTA\text{-}P2]) = PB_{max} / (1+(IC_{50} / [TTA\text{-}P2])^{n}) \quad (1)$$

where PB_{max} is the maximal percent block of peak current, IC_{50} is the concentration that produces 50% inhibition, and *n* is the apparent Hill coefficient for blockade. The fitted value is reported with 95% linear confidence limits. The voltage dependencies of activation and steady-state inactivation were described with single Boltzmann distributions of the following forms:

$$\text{Activation:} \quad G(V) = G_{max} / (1+\exp [-(V-V_{50}) / k]) \quad (2)$$

$$\text{Inactivation:} \quad I(V) = I_{max} / (1+\exp [(V-V_{50}) / k]) \quad (3)$$

In these forms, I_{max} is the maximal amplitude of current; G_{max} is the maximal conductance; V_{50} is the voltage at which half of the current is activated or inactivated; and *k* represents the voltage dependence (slope) of the distribution.

The time course of macroscopic T-current inactivation and deactivating tail currents were fitted using a single-exponential equation: $y = A_1 * e^{(-x / \tau 1)} + y_0$, where A_1 is the amplitude and τ_1 the decay constant and y_0 the offset. (4)

Molecular Pharmacology Fast Forward. Published on August 5, 2011 as DOI: 10.1124/mol.111.073205
This article has not been copyedited and formatted. The final version may differ from this version.

For fitting the time course of recovery from inactivation, a double exponential function was used, yielding two time constants (τ1 and τ2) and their corresponding amplitudes (A1 and A2). (5)

TTA-P2 was prepared as 100-300 mM stock solutions in DMSO. The final concentrations of DMSO had no significant effect on T-current amplitude in DRG and HEK 293 cells (data not shown).

The external solution used to isolate T-currents contained, in mM, 2 $CaCl_2$, 152 TEA-Cl, and 10 HEPES adjusted to pH 7.4 with TEA-OH. To minimize contamination of T-currents with even minimal HVA components, we used only fluoride (F^-)-based internal solution to facilitate high-voltage-activated (HVA) calcium current rundown; this solution contained, in mM, 135 tetramethylammonium hydroxide (TMA-OH), 10 EGTA, 40 HEPES, and 2 $MgCl_2$, adjusted to pH 7.2 with hydrofluoric acid (HF). This allowed studies of well-isolated and well-clamped T-currents in small DRG cells. All chemicals were obtained from Sigma (St. Louis, MO) unless otherwise noted. Statistical comparisons were made, where appropriate, using an unpaired Student t-test, Mann-Whitney sum test, and chi-square test. All quantitative data are expressed as means of multiple experiments $\pm$ standard error of the mean (SEM) unless stated otherwise. The amplitude of T-current was measured from the peak, which was subtracted from the current at the end of the depolarizing test potential to avoid contamination with residual HVA currents that were present at more positive membrane potentials (typically -20 mV and higher). To record HVA calcium currents in DRG and HEK cells, we used the same external solution except that equimolar $BaCl_2$ was substituted for $CaCl_2$ and the internal solution contained, in mM, 110 Cs-methane sulfonate, 14 phosphocreatine, 10 HEPES, 9 EGTA, 5 Mg-ATP, and 0.3 tris-GTP, adjusted to pH 7.3 with CsOH. For recordings of

Molecular Pharmacology Fast Forward. Published on August 5, 2011 as DOI: 10.1124/mol.111.073205
This article has not been copyedited and formatted. The final version may differ from this version.

voltage-gated sodium currents in DRG cells, we used the same fluoride-based internal solution as for recordings of T-currents. The external solution contained, in mM, 140 NaCl, 4 KCl, 2 $MgCl_2$, 2 $CaCl_2$, 0.5 $CdCl_2$, 10 glucose, and 10 HEPES, adjusted to pH 7.4. In some experiments, this solution was supplemented with 1 μM tetrodotoxin (TTX).

II. In vivo studies

Chemicals and animals: In all experiments, Sprague-Dawley adult female rats (retired breeders) and adult C57BL6 mice of both sexes were used. Streptozocin (STZ) was purchased from Sigma (St. Louis, MO). Antisense oligonucleotides and mismatched oligonucleotides (using the sequence previously published by Bourinet et al., 2005; Messinger et al., 2009) were purchased from Invitrogen (Carlsbad, CA). Antisense-$Ca_V3.2$ (AS): CCACCTTCTTACGCCAGCGG, which was used to knock down the T-type-channel pore-forming subunit of the gene encoding the α1H ($Ca_v3.2$) or Mismatch-$Ca_V3.2$ (Mis-$Ca_V3.2$; MIS): TACTGTACTTGCGAGGCCAC were dissolved in sterile neutral pH buffer solution. Vehicle experiments were performed using sterile saline neutral pH buffer solution. As in previous studies (Messinger et al., 2009), vehicle and MIS were found to have no effect on thermal nociception.

TTA-P2 was kindly provided by Dr. John Renger and Dr. Victor N. Uebele (MERCK Res. Lab., West Point, PA). For all of our *in vivo* studies TTA-P2 was dissolved in 15% cyclodextrin and injected intraperitoneally (i.p.) at the doses of 5mg/kg, 7.5 mg/kg or 10 mg/kg. Cyclodextrin [(2-hydroxypropyl)-β-cyclodextrin solution (Sigma, St. Louis, MO) was balanced at pH 7.4 just before injection.

Induction of PDN with streptozocin: All experimental protocols were approved by the University of Virginia Animal Care and Use Committee and were in accordance with

Molecular Pharmacology Fast Forward. Published on August 5, 2011 as DOI: 10.1124/mol.111.073205
This article has not been copyedited and formatted. The final version may differ from this version.

the *Guide for the Care and Use of Laboratory Animals* (NIH). All possible efforts were made to minimize animals' suffering and to minimize the number of animals used.

To induce peripheral diabetic neuropathy (PDN), we intravenously (i.v.) injected freshly dissolved streptozocin (STZ) solution at pH 5-6, using a dose of 50 mg/kg. This dose causes severe hyperglycemia and pain-like behavior within the first few days after injection, but does not cause severe generalized sickness (e.g., ketoacidosis, malaise, wasting) (Aley and Levine , 2001; Jagodic et al., 2007; Messinger et al., 2009). Control rats received the same volume/kg of i.v. sterile saline. The animals were studied for 10 days after the day of i.v. injection.

Three days after injecting STZ (or saline), at which point STZ-injected rats had developed PDN, we intrathecally (i.t.) injected 12.5 μg/25 μl of either $Ca_V3.2$ antisense oligonucleotides (AS) or mismatch (MIS) (or 25 μl of saline-SAL) into the L_{5-6} region of the spinal cord every 12 h for 4 days (a total of 8 injections) to test the effects of oligonucleotides. All solutions were pH balanced to 7.4 to avoid spinal cord irritation. Rats were maintained in a surgical plane of anesthesia with isoflurane (2%-3% in oxygen delivered via nose cone) throughout the injection procedure. We previously showed that i.t. injections as described lead to preferential uptake of AS by DRG sensory neurons and minimal uptake by spinal cord tissues (Messinger et al., 2009). This method of AS application reliably reversed neuropathic hyperalgesia in diabetic rats and concomitantly reversed up-regulation of T-currents in rat sensory neurons, while injections of saline or MIS i.t. in the same manner did not affect pain responses and T-current density in DRG cells (Messinger et al., 2009).

III. *Behavioral studies:*

Molecular Pharmacology Fast Forward. Published on August 5, 2011 as DOI: 10.1124/mol.111.073205
This article has not been copyedited and formatted. The final version may differ from this version.

Assessment of thermal sensitivity: The nociceptive response to thermal stimulation was measured using a paw thermal stimulation system consisting of a clear plastic chamber (10 x 20 x 24 cm) that sits on a clear elevated glass floor and is temperature regulated at 30°C. As previously described (Messinger et al., 2009), each rat is placed in the plastic chamber for 15 min to acclimate. A radiant heat source mounted on a movable holder beneath the glass floor is positioned to deliver a thermal stimulus to the plantar side of the hind paw. When the rat withdraws the paw, a photocell detects interruption of a light beam reflection and the automatic timer shuts off. This method has a precision of ± 0.05 sec for the measurement of paw withdrawal latency (PWL). To prevent thermal injury, the light beam is automatically discontinued at 20 sec if the rat fails to withdraw its paw. Pain testing was done before STZ or vehicle injection (day 0) and daily thereafter for up to 10 days. The stability of daily pain recordings was confirmed by saline-injected controls.

Statistical analysis: PWLs were subjected to analysis of variance (ANOVA) containing one within-subject variable, test session (before the administration of STZ or vehicle versus each posttreatment day up to 10 days), and one between-subject variable, AS versus TTA-P2. Relevant pairwise comparisons were done and alpha levels were adjusted using the Bonferroni procedure when appropriate.

Assessment of inflammatory pain in mice: Behavioral tests for inflammatory pain after formalin injection were done with mice in a clear plexiglass chamber prefilled with air at a flow of 6 L/min, as we recently reported (Orestes et al., 2011). Each mouse was first placed in the prefilled chamber to accommodate for 30 min, then removed from the chamber, injected in the plantar side of the right paw with 20 µl of 5% formalin or vehicle (15% cyclodextrin) and returned to the test chamber. The time in seconds that the mouse spent licking and biting the paw was measured for an hour and recorded per every 5-min interval. Afterward, the mouse's temperature was measured to ensure

Molecular Pharmacology Fast Forward. Published on August 5, 2011 as DOI: 10.1124/mol.111.073205
This article has not been copyedited and formatted. The final version may differ from this version.

normothermia. To test the effects of TTA-P2, a mouse was injected i.p. with fresh TTA-P2 solution (5 or 7.5 mg/kg) or an equal volume of vehicle. Thirty min later, the mouse was placed inside the chamber to equilibrate and become familiar with the environment. One hour after the injection of TTA-P2 or vehicle, the mouse was injected with formalin. The rest of the experiment was performed as described in the preceding section.

Assessment of sensorimotor abilities: The sensorimotor battery in mice consisted of three tests, the ledge, platform, and inclined screen. These tests are designed to assess agility and fine motor abilities, as we described in a recent publication (Latham et al., 2009).

RESULTS

The *in vitro* results presented here were obtained from a total of 144 small DRG cells having an average soma diameter of 25 ± 3 μm (mean ± SD) and an average membrane capacitance of 24 ± 4 pF (mean ± SD). We began our study by testing the effects of TTA-P2 on well-isolated T-currents in rat sensory neurons. Traces (Fig. 2A) and time course (Fig. 2B) from the same representative DRG cell indicate that at 1 μM, TTA-P2 inhibited most of the T-current that was recorded at holding potentials (V_h) of -90 mV. Figure 2B shows that the inhibitory effect of TTA-P2 had a fast onset, but was slowly and only partially reversible. Interestingly, similarly fast onset and slow reversibility of the inhibition of T-currents with TTA-P2 in thalamic relay neurons has also been reported (Dreyfus et al., 2010). Furthermore, the traces shown in Fig. 2C demonstrate that TTA-P2 at 10 μM had little effect (less than 10%) on the amplitude of HVA Ca^{2+} currents in acutely dissociated DRG cells. For recordings of HVA currents, cells were held at -50 mV in order to separate that signal from T-currents that are almost completely inactivated at positive membrane potentials.

Molecular Pharmacology Fast Forward. Published on August 5, 2011 as DOI: 10.1124/mol.111.073205
This article has not been copyedited and formatted. The final version may differ from this version.

Some of the calcium channel blockers thought to be selective for T-currents (e.g. mibefradil, nickel, ethosuximide) may also affect the R-type ($Ca_V2.3$) subtype of HVA calcium currents in the same concentration range (Randall and Tsien, 1997; Nakashima et al., 1998). The above studies have also shown that separation of T-currents from R-type currents in native cells is further complicated by the fact that they appear to inactivate at somewhat comparable rates. Thus, we tested the ability of TTA-P2 to inhibit human recombinant $Ca_V2.3$ channels stably co-expressed with β3 calcium channel subunits in human embryonic kidney (HEK) 293 cells (Nakashima et al., 1998). Traces from a representative HEK 293 cell shown in Fig. 2D demonstrate that TTA-P2 at 10 μM inhibited only about 10% of the recombinant $Ca_V2.3$ current. We also tested the ability of TTA-P2 to inhibit voltage-gated sodium currents (I_{Na+}), since these channels are critical regulators of the excitability of nociceptive sensory neurons and are implicated in neuropathic pain (Dib-Hajj et al., 1999; Lai et al., 2002; Hong et al., 2004). Traces from representative DRG cells shown in Fig. 2E demonstrate that 1 μM TTA-P2 had little effect on the amplitude of total voltage-gated sodium currents (I_{Na+}, left panel) or the tetrodoxin-resistant component of voltage-gated sodium currents ($I_{Na+TTXR}$, right panel). On average, the effects of 1 μM TTA-P2 on the amplitude of DRG sodium currents were as follows: total I_{Na+} 1 ± 4% change ($p > 0.05$, $n = 8$) and, similarly, 1 ± 7% change of $I_{Na+TTXR}$ ($p > 0.05$, $n = 5$). To compare the potency of TTA-P2 in inhibiting T-currents and HVA-currents in DRG cells, as well as recombinant $Ca_V2.3$ currents, we obtained multiple points on concentration-response relationships and generated best fits using equation 1 (Fig. 3). These experiments indicated, impressively, that TTA-P2 was 2-3 orders of magnitude more potent in inhibiting DRG T-currents (solid circles, IC_{50} about 100 nM) than it was in inhibiting total DRG HVA-currents (solid squares, IC_{50} about 165 μM) and recombinant $Ca_V2.3$ currents (open triangles, IC_{50} about 35 μM).

Molecular Pharmacology Fast Forward. Published on August 5, 2011 as DOI: 10.1124/mol.111.073205
This article has not been copyedited and formatted. The final version may differ from this version.

We then set out to discern the biophysical mechanisms of T-current inhibition by TTA-P2, which could contribute to the inhibition of current and consequently diminish the cellular excitability of DRG cells. To determine the effects of TTA-P2 on the kinetic properties of DRG T-currents, we measured current-voltage (I-V) relationships in the presence and absence of 0.1 μM TTA-P2 (Fig. 4A), finding that, as compared to controls (open symbols), TTA-P2 (filled symbols) reduced T-current amplitudes at all test potentials between –50 and -20 mV (Fig. 4B), but had little effect on the kinetics of macroscopic current inactivation or activation (Fig. 4C and 4D, respectively). The only significant effect was that TTA-P2 slowed 10%-90% rise time at test potential of -40 mV for about 50% (Fig. 4D). Similarly, TTA-P2 did not induce significant alterations of channel gating, as shown by similar half-maximal activation (V_{50}) of the T-channels before and during drug application (Fig. 4E). Interestingly, TTA-P2 decreased the rate of channel closure after repolarization, as demonstrated by significantly slower deactivation time constants (τs) at -130, -120, -110 and -100 mV (Fig. 4F). Binding to inactivated states and off-rate of the compound are important properties of drugs that modulate ion channels since it allows them to have tissue selectivity based on the different membrane potential cycling conditions. Transitions from closed to inactivated states can be measured using long prepulses at different potentials, producing what are commonly referred to as steady-state inactivation curves. We assessed steady-state inactivation curves using a standard double-pulse protocol with 3.6 s-long prepulses to variable voltages (from -110 to -45 mV) and test potentials to -30 mV. As shown in Figures 5A and 5B, TTA-P2 (solid symbols), as compared to control conditions (open symbols), had a great effect on the voltage-dependent kinetics of channel inactivation, as determined by a hyperpolarizing shift in steady-state inactivation curves of about 20 mV. These data suggest that TTA-P2 binds to and stabilizes inactive states of the channel and thus is a

Molecular Pharmacology Fast Forward. Published on August 5, 2011 as DOI: 10.1124/mol.111.073205
This article has not been copyedited and formatted. The final version may differ from this version.

more potent blocker at depolarized membrane potentials. For example, it is evident in Fig. 5A that 100 nM TTA-P2 inhibits about 40% of maximal T-current at -110 mV, while the same concentration inhibits T-current almost 100% at -65 and -60 mV. T-channels can recover from inactivation during sufficiently long hyperpolarizations of the neuronal membrane caused by the effects of neuromodulators like serotonin in DRG neurons (Nelson et al., 2005). This can drastically influence firing properties of cells that express T-channels. Thus, we studied the effects of 100 nM TTA-P2 on recovery from inactivation using our standard double-pulse protocol with variable inter-pulse duration at -90 mV (Fig. 5C) after 500 msec-long inactivating pulse (V_h -90 mV, V_t -30 mV). Figure 5C depicts these data indicating that in the presence of TTA-P2 (black squares) T-currents recover partially to only about 60% of the T-current amplitudes of pre-drug control values (open circles). The hyperpolarizing shift in steady-state inactivation and incomplete recovery from inactivation could be highly useful properties for a channel inhibitor since, when applied *in vivo*, it will affect actively firing neurons more potently than it will resting cells. Thus, we tested the efficacy of TTA-P2 in two frequently used animal models of pain.

Previous studies with $Ca_V3.2$ knock-out mice have established the role of T-channels in inflammatory pain (Choi et al, 2007). Thus, to explore the interaction of TTA-P2 and T-channels *in vivo*, we used injections of formalin into the hind paws of mice to measure inflammatory pain. The amount of time mice spend licking and biting the injected paw in the first five minutes after injection is a response to direct activation of peripheral nociceptors (phase 1, P1). In contrast, responses 10-60 min after injection reflects central sensitization of pain (phase 2, P2). As shown in Figure 6A, TTA-P2 at 7.5 mg/kg i.p. (solid gray columns) when compared to vehicle controls (solid black columns) significantly reduced licking and biting of the affected paws in P1, P2, and total time from 30% up to 50%. When TTA-P2 was injected at a dose of 5 mg/kg i.p., mice

Molecular Pharmacology Fast Forward. Published on August 5, 2011 as DOI: 10.1124/mol.111.073205
This article has not been copyedited and formatted. The final version may differ from this version.

demonstrated somewhat reduced, but not significant (about 20%), analgesia in P1, while total time and P2 were significantly decreased by about 50% (open symbols, Fig. 6A).

We also considered the possibility that TTA-P2 might nonspecifically decrease pain responses by inducing a general depression of behavioral performance. To determine whether TTA-P2, given at its effective analgesic doses in mice of 5 or 7.5 mg/kg, causes sensorimotor disturbances such as motor weakness or sedation, which could affect the validity of behavioral sensory testing, we did a battery of sensorimotor tests focused on agility and fine motor abilities (Latham et al., 2009). Mice were tested using an inclined plane (Fig. 6B left panel), platform (Fig. 6B middle panel), and ledge (Fig. 6B, right panel) before TTA-P2 injection and at 60 min after injection. The responses of mice treated with 5 mg/kg of TTA-P2 (open bars) or 7.5 mg/kg of TTA-P2 (gray bars) did not significantly differ from these mice's responses before injection (black bars) on any of the tests, indicating that the effect of TTA-P2 on alleviation of inflammatory pain is unlikely to result from sedation or motor impairment.

Our recent studies have established that T-channels are up-regulated in putative nociceptive sensory neurons of diabetic rats treated with streptozocin (STZ) and that this up-regulation may increase the cellular excitability of these neurons (Jagodic et al., 2007). Furthermore, we used specific *in vivo* knockdown of the most prevalent isoform of T-channels in DRG sensory neurons, $Ca_V3.2$, to alleviate neuropathic pain in STZ-treated diabetic rats (Messinger et al., 2009). We first asked whether pharmacological antagonism of T-channels with TTA-P2 could reverse thermal hypersensitivity in diabetic rats treated with STZ. As shown in the top panel of Figure 7, incremental doses of TTA-P2 at 5, 7.5, or 10 mg/kg did not change baseline pain responses (B) in either right paws (open symbols) or left paws (filled symbols) of control animals. When the same doses of TTA-P2 were injected into diabetic STZ-treated rats with neuropathic hyperalgesia as demonstrated by about a 30% reduction in thermal PWLs, there was progressive

Molecular Pharmacology Fast Forward. Published on August 5, 2011 as DOI: 10.1124/mol.111.073205
This article has not been copyedited and formatted. The final version may differ from this version.

alleviation of pain (Fig. 7, middle panel). At 10 mg/kg of TTA-P2 i.p., there was a complete reversal of neuropathic hyperalgesia as demonstrated by apparent normalization of thermal PWLs. In control experiments, the same volume of vehicle injected into diabetic rats i.p. did not significantly affect PWLs: right-paw controls, 6.9 ±1.3 sec, vehicle 6.9 ± 0.4 sec; left-paws control, 7.6 ± 2.3 sec, vehicle 6.5 ± 0.5 sec ($p > 0.5$, $n = 3$, data not shown). We next asked whether the efficacy of TTA-P2 could be mediated by off-target activity in diabetic rats. We reasoned that if TTA-P2-induced reversal of thermal hypersensitivity in diabetic rats is specifically mediated by the inhibition of T-channels *in vivo*, then we should be able to abolish or at least greatly diminish any analgesic effects of TTA-P2 with knockdown of $Ca_V3.2$ in sensory neurons. Indeed, we found that pretreatment with specific antisense (AS) against $Ca_V3.2$ in diabetic rats completely reversed diabetic hyperalgesia when given alone. When AS against $Ca_V3.2$ was administered concomitantly with TTA-P2 at 5, 7.5 or 10 mg/kg i.p., it did not significantly affect new baselines in either right or left paws (Fig. 7, bottom panel). In control experiments, we injected morphine (i.p., 10 mg/kg) in AS and MIS treated diabetic rats and assessed its effect on thermal nociceptive responses at 1 hour post-injection. We found that morphine similarly decreased thermal nociceptive responses in both AS (left paws 7.2±0.9 sec and right paws 7.4±0.3 sec increase in PWLs from baselines) and MIS treated groups (left paws 7.5±0.4 sec and right paws 6.9±0.9 sec increase in PWLs from baselines), ($n=3$ per group, $p>0.05$, data not shown). This strongly suggests that abolished anti-hyperalgesic effect of TTA-P2 in AS-treated diabetic rats is not due to decreased basal pain responses. Diabetic rats did not appear to be less active than control ones in spite of some weight loss and severe hyperglycemia. Furthermore, although daily weights and blood glucose (BG) levels of rats treated with STZ and STZ+AS were different from baseline, they were not significantly different in the two treatment groups: Baseline weight, 308 ± 7 gm; STZ

Molecular Pharmacology Fast Forward. Published on August 5, 2011 as DOI: 10.1124/mol.111.073205
This article has not been copyedited and formatted. The final version may differ from this version.

group, 280 ± 6 gm; STZ+AS group, 275 ± 8 gm; n = 6. Baseline BG: 84 ±4 mg/dl,; STZ group, 423 ± 39 mg/dl; STZ+AS group, 464 ± 40 mg/dl; n = 6. Thus, it appears that inhibition of $Ca_V3.2$ channels is the main mechanism that regulates TTA-P2-mediated anti-hyperalgesia in diabetic rats.

DISCUSSION

In this study, we demonstrated that the new compound TTA-P2 is a potent and selective blocker of T-currents in rat sensory neurons *in vitro* and a highly potent antinociceptive agent in two animal models of pain *in vivo*. The potency of TTA-P2 in inhibiting native DRG T-current (IC_{50} of 100 nM) is close to that previously reported for inhibition of the recombinant Ca_V3 currents $Ca_V3.1$ 93 nM, $Ca_V3.2$ 196 nM, and $Ca_V3.3$ 84 nM (Shipe et al., 2008). Indeed, we found that TTA-P2 in DRG cells even at 100-fold higher concentrations has little effect on other voltage-gated currents in sensory neurons. We also found that TTA-P2 inhibited DRG T-currents in a voltage-dependent manner. Figure 4 summarizes our biophysical experiments, which indicate that TTA-P2 induced mild slowing of channel closure after brief depolarizations (deactivation), while it had a minimal effect on channel gating, as well as macroscopic inactivation and activation rates.

Importantly, the results shown in Figure 5 indicate that TTA-P2 caused a marked voltage-dependent blockade of T-channels, as demonstrated by a large hyperpolarizing shift of the steady-state inactivation curve. This voltage dependence indicates the drug's preference for inactive states of the channel, resulting in higher fractional block of the channel at depolarized membrane potentials. This is in contrast to mechanisms of inhibition in thalamic relay neurons in brain slices, where TTA-P2 acts as a state-independent antagonist of T-channels (Dreyfus et al., 2010). However, it is possible that

Molecular Pharmacology Fast Forward. Published on August 5, 2011 as DOI: 10.1124/mol.111.073205
This article has not been copyedited and formatted. The final version may differ from this version.

the difference between the mechanisms of channel inhibition in native thalamic and sensory neurons is due to the expression of different T-channel isoforms in thalamic relay neurons ($Ca_V3.1$) and DRG cells ($Ca_V3.2$). Our finding is somewhat unexpected, given that a previous study found that recombinant $Ca_V3.2$ channel were also inhibited by TTA-P2 in a voltage-independent manner (Shipe et al., 2008). In contrast, the structurally unrelated compound TTA-A2 shows state-dependent features of recombinant T-channel inhibition (Kraus et al., 2010). It is possible that different splice variants of $Ca_V3.2$ are expressed in adult DRG cells; alternatively, another unknown ancillary subunit that can modify the interaction of TTA-P2 with T-channels may be co-expressed in DRG cells. It is noteworthy that we have also described substantial differences in the mechanism of T-channel blockade of native DRG cells and recombinant $Ca_V3.2$ channels for the anticonvulsants phenytoin and succinimide (Todorovic et al., 2000).

Additional molecular studies will be needed to resolve this issue. However, regardless of the precise basis for differences in the observations, voltage-dependent inhibition of the channel may be useful for clinical applications of TTA-P2, since it appears preferably to inhibit the neuronal excitability of actively firing DRG cells. This effect may explain the selective reversal of neuropathic hyperalgesia in diabetic rats with a dose that was completely ineffective in naive rats (Fig. 7). Thus, lowering the dose of drug used *in vivo* may greatly decrease the risk of adverse side effects. It is also important to note that some *in-vitro* studies reported prominent expression of $Ca_V3.2$ T-currents in non-nociceptive subpopulations of putative mechanosensitive DRG cells (Dubreuil et al., 2004; Coste et al., 2007). However, to our knowledge the role of T-channels in mechanosensation has not been validated *in vivo*.

The analgesic effect of TTA-P2 in the formalin inflammatory pain model in mice and antihyperalgesic effect in diabetic rats are achieved at concentrations of 5-10 mg/kg

Molecular Pharmacology Fast Forward. Published on August 5, 2011 as DOI: 10.1124/mol.111.073205
This article has not been copyedited and formatted. The final version may differ from this version.

(Figs. 6-7). Previous pharmacokinetic studies in rodents and other species have shown that at these doses plasma concentrations of TTA-P2 reach 0.2-1.0 μM and that TTA-P2 penetrates well into the CNS (Shipe et al., 2008). These findings strongly suggest that the analgesic and antihyperalgesic effects of TTA-P2 observed in our study could be related to the pharmacological antagonism of T-currents in peripheral sensory neurons, the CNS, or both. Importantly, we directly implicated the $Ca_V3.2$ isoform of T-channels in the effects of TTA-P2 in diabetic neuropathic pain by demonstrating that injections of antisense oligonucleotides specific for $Ca_V3.2$ completely abolished effects of TTA-P2 on thermal PWLs (Fig. 7).

Our study strongly suggests that TTA-P2 is more suitable for functional studies than are many currently available compounds thought to be selective T-channel blockers. By virtue of their unique activation, deactivation, and inactivation properties, T-currents are relatively easy to study *in vitro* in isolation from other calcium current components. However, pharmacological tools for identifying and investigating T-currents have been very limited. For example, it was reported that a scorpion toxin, kurtoxin, potently blocks recombinant T-currents at nanomolar range with an IC_{50} for $Ca_V3.1$ of 15 nM (Chuang et al, 1998). However, kurtoxin has limited usefulness because it also blocks voltage-gated Na^+ currents and native HVA currents within the same concentration range (Chuang et al., 1998; Sidach and Mintz 2002). Of the other described compounds with known effects on T-currents, including traditional agents such as ethosuximide (Coulter et al., 1989) and amiloride (Tang et al., 1988), most are reported to block with an IC_{50} in excess of 100 μM. At these concentrations, effects on other ion channels also occur, raising questions about the usefulness of these agents as specific probes of T-current function. Among the other available pharmacological agents, nickel at low micromolar concentrations (Lee et al., 1999) and gaseous

Molecular Pharmacology Fast Forward. Published on August 5, 2011 as DOI: 10.1124/mol.111.073205
This article has not been copyedited and formatted. The final version may differ from this version.

anesthetic/analgesic nitrous oxide up to 80% (Todorovic et al., 2001) can be used for selective definition of $Ca_V3.2$ T-currents as opposed to other Ca_V3 currents. However, at similar concentrations, nickel blocks $Ca_V2.3$ R-type HVA currents (Zamponi et al., 1996), while nitrous oxide inhibits N-methyl-D-aspartate receptors (NMDA) in the CNS (Jevtovic-Todorovic et al., 1998).

Some new experimental agents are more promising in selectively targeting T-channels. We have previously reported that a neuroactive steroid with a 5α configuration at the steroid A,B ring fusion [(+)-ECN] is a potent, voltage-dependent, but only partial blocker of T-channels in rat sensory neurons (IC_{50} of 300 nM, maximal block 40%) (Todorovic et al., 1998). Also, we recently described another novel steroid, a voltage-dependent blocker of T-channels in rat sensory neurons; it has a 5β configuration at the steroid A,B ring fusion (3βOH), which more completely blocks T- currents, but with decreased potency with an IC_{50} of 2.8 μM (Todorovic et al., 2004). Moreover, our previous studies have documented that both ECN and 3βOH are about 10-fold more potent in inhibiting T-type currents than in inhibiting HVA currents in rat sensory neurons (Todorovic et al., 1998; 2004). In comparison with neuroactive steroids, it appears that TTA-P2 is even more potent and more selective in inhibiting T-currents in DRG cells, and thus is a better tool for the study of these channels. Although no preclinical data are currently available on the long-term use of ECN and related neuroactive steroids, evaluation of the safety of TTA compounds in dogs has disclosed no cardiovascular or renal side effects (Shipe et al., 2008).

This study confirms our previously published conclusion that T-channel blockers are important and novel agents for the treatment of pain disorders. No presently available treatments can completely reverse the significantly adverse effects of intractable pain on quality of life measures. We hope that our studies may inspire future clinical trials that

Molecular Pharmacology Fast Forward. Published on August 5, 2011 as DOI: 10.1124/mol.111.073205
This article has not been copyedited and formatted. The final version may differ from this version.

will lead to better treatments for intractable inflammatory pain and, in particular, the painful symptoms of patients with peripheral diabetic neuropathy.

AUTHORSHIP CONTRIBUTION

Participated in research design: SMT, VJT, RS, RBM, and WJC.

Conducted experiments: RS, RBM, V-SE, WJC, AO and EL.

Performed data analysis: SMT, RBM, AO and EL.

Wrote and contributed to the writing of the manuscript: SMT and VJT.

Molecular Pharmacology Fast Forward. Published on August 5, 2011 as DOI: 10.1124/mol.111.073205
This article has not been copyedited and formatted. The final version may differ from this version.

REFERENCES

Aley KO and Levine JD (2001) Rapid onset pain induced by intravenous streptozotocin in the rat. *J Pain* **2**:146-50.

Beedle AM, McRory JE, Poirot O, Doering CJ, Altier C, Barrere C, Hamid J, Nargeot J, Bourinet E and Zamponi GW (2004) Agonist-independent modulation of N-type calcium channels by ORL1 receptors. *Nat Neurosci* **7**: 118–125.

Bhave G and Gereau RW (2004) Posttranslational mechanisms of peripheral sensitization. *J Neurobiol* **61**:88-106.

Bourinet E, Alloui A, Monteiol A, Barrere C, Couette B, Poirot O, Pages A, McRory J, Snutch TP, Eschalier A and Nargeot J (2005) Silencing of the $Ca_v3.2$ T-type calcium channel gene in sensory neurons demonstrates its major role in nociception. *EMBO J* **24**: 315-324.

Campbell JN and Meyer RA (2006) Mechanisms of neuropathic pain. *Neuron* **52**: 77-92.

Choi S, Na HS, Kim J, Lee J, Lee S, Kim D, Park J, Chen CC, Campbell KP and Shin HS. Attenuated pain responses in mice lacking CaV3.2 T-type channels. *Genes Brain Behav* **6**: 425-431.

Chuang RSI, Jaffe H, Cribbs L, Perez-Reyess E and Swartz KJ (1998) Inhibition of T-type voltage-gated calcium channels by a new scorpion toxin. *Nat Neurosci* **1(8)**:668-674.

Clozel J-P, Ertel EA and Ertel SI (1997) Discovery and main pharmacological properties of mibefradil (Ro 40-5967), the first selective T-type calcium channel blocker. *J Hypertension Supplement* **15**: S17-S25.

Coderre TJ, Katz J, Vaccarino AL and Melzack R (1993). Contribution of central neuroplasticity to pathological pain: review of clinical and experimental evidence. *Pain* **52**: 259-285.

Coste B, Crest M and Delmas P (2007) Pharmacological dissection and distribution of NaN/Nav1.9, T-type Ca2+ currents, and mechanically activated cation currents in different populations of DRG neurons. *J Gen Physiol* **129(1)**: 57-77.

Cribbs LL, Lee J, Yang J, Satin J, Zhang Y, Daud A, Barcley J, Williamson MP, Fox M, Rees M and Perez-Reyes E (1998) Cloning and characterization of α1H from human heart, a member of the T-type Ca^{2+} channel gene family. *Circ Res* **83**: 103-109.

Dib-Hajj SD, Fjell J, Cummins TR, Zheng Z, Fried K, LaMotte R, Black JA and Waxman SG (1999) Plasticity of sodium channel expression in DRG neurons in the chronic constriction injury model of neuropathic pain. *Pain* **83(3)**:591-600.

Dogrul A, Gardell LR, Ossipov MH, Tulunay FC, Lai J and Porecca F (2003) Reversal of experimental neuropathic pain by T-type calcium channel blockers. *Pain* **105**:159-168.

Dreyfus FM, Tscherter A, Errington AC, Renger JJ, Shin HS, Uebele VN, Crunelli V, Lambert RC and Leresche N (2010) Selective T-type calcium channel block in thalamic neurons reveals channel redundancy and physiological impact of I(T)window. *J Neurosci* **30(1)**:99-109.

Dubreuil AS, Boukhaddaoui H, Desmadryl G, Martinez-Salgado C, Moshourab R, Lewin GR, Carroll P, Valmier J and Scamps F (2004) Role of T-type calcium current in identified d-hair mechanoreceptor neurons studied in vitro. *J Neurosci* **24**: 8480–8484.

Edwards JL, Vincent AM, Cheng HT and Feldman EL (2008) Diabetic neuropathy: mechanisms to management. *Pharmacology & Therapeutics* **120**:1-34.

Gooch C and Podwall D (2004) The diabetic neuropathies. *The Neurologist* **10**: 311-322.

Hong S, Morrow TJ, Paulson PE, Isom LL and Wiley JW (2004) Early painful diabetic neuropathy is associated with differential changes in tetrodotoxin-sensitive and -resistant sodium channels in dorsal root ganglion neurons in the rat. *J Biol Chem* **279**:29341-50.

Jagodic MM, Pathirathna S, Joksovic PM, Lee W, Nelson MT, Naik AK, Su P, Jevtovic-Todorovic V and Todorovic SM (2008) Up-regulation of the T-type calcium current in small rat sensory neurons after chronic constrictive injury of the sciatic nerve. *J Neurophysiol* **99**: 3151-3156.

Jagodic MM, Pathirathna S, Nelson MT, Mancuso S, Joksovic PM, Rosenberg ER, Bayliss DA, Jevtovic-Todorovic V and Todorovic SM (2007) Cell-specific alterations of T-type calcium current in painful diabetic neuropathy enhance excitability of sensory neurons. *J Neurosci* **27**: 3305-3316.

Jevtovic-Todorovic V and Todorovic SM (2006) The role of peripheral T-type calcium channels in pain transmission. *Cell Calcium* **40(2)**:197-203.

Jevtovic-Todorovic V, Todorovic SM, Mennerick S, Powell S, Dikranian K, Benshoff N, Zorumski CF and Olney JW (1998) Nitrous oxide (laughing gas) is an NMDA antagonist, neuroprotectant and neurotoxin. *Nat Med* **4**: 460–463.

Kim D, Park D, Choi S, Lee S, Sun M, Kim C and Shin HS (2003) Thalamic control of visceral nociception mediated by T-type Ca^{2+} channels. *Science* **302**: 117–119.

Kraus RL, Li Y, Gregan Y, Gotter AL, Uebele VN, Fox SV, Doran SM, Barrow JC, Yang ZQ, Reger TS, Koblan KS and Renger JJ (2010). In vitro characterization of T-type calcium channel antagonist TTA-A2 and in vivo effects on arousal in mice. *J Pharmacol Exp Ther* **335**(2):409-17.

Lai J, Gold MS, Kim CS, Bian D, Ossipov MH, Hunter JC and Porreca F (2002) Inhibition of neuropathic pain by decreased expression of the tetrodotoxin-resistant sodium channel, NaV1.8. *Pain* **95**: 143−152.

Latham JR, Pathirathna S, Jagodic MM, Choe WJ, Levin ME, Nelson MT, Lee WY, Krishnan K, Covey D, Todorovic SM and Jevtovic- Todorovic V (2009) Selective T-type calcium channel blockade alleviates hyperalgesia in ob/ob mice. *Diabetes* **58(11)**:2656-65.

Lee JH, Daud AN, Cribbs LL, Lacerda AE, Pereverzev A, Klockner U, Schneider T and Perez-Reyes E (1999) Cloning and expression of a novel member of the low voltage-activated T-type calcium channel family. *J Neurosci* **19**: 1912-1921.

Lee JH, Gomora JC, Cribbs LL and Perez-Reyes E (1999) Nickel block of three cloned T-type calcium channels: low concentrations selectively block alpha1H. *Biophys J* **77(6)**:3034-42.

Leresche N, Parri HR, Erdemli G, Guyon A, Turner JP, Williams SR, Asprodini E and Crunelli V (1998) On the action of the anti-absence drug ethosuximide in the rat and cat thalamus. *J Neurosci* **18(13)**:4842-53.

Lory P and Chemin J. Towards the discovery of novel T-type calcium channel blockers. *Expert Opin Ther Targets* **11(5)**:717-22.

McCleskey EW and Gold MS (1999) Ion channels of nociception. *Annu Rev Physiol* **61**: 835-856.

McGivern JG (2006) Pharmacology and drug discovery for T-type calcium channels. *CNS Neurol Disord Drug Targets* **5(6)**:587-603.

Messinger RB, Naik AK, Jagodic MM, Nelson MT, Lee WY, Choe WJ, Orestes P, Latham, JR, Todorovic SM and Jevtovic-Todorovic V (2009) In-vivo silencing of the Cav3.2 T-type calcium channels in sensory neurons alleviates hyperalgesia in rats with streptozocin-induced diabetic neuropathy. *Pain* **145**: 184-195.

Nakashima YM, Todorovic SM, Pereverzev A, Heschler J, Schneider T and Lingle CJ (1998) Properties of Ca^{2+} currents arising from human α_{1E} and $\alpha_{1E}\beta_3$ constructs

expressed in HEK293 cells: physiology, pharmacology, and comparison to native T-type Ca^{2+} currents. *Neuropharmacology* **37**:957-972.

Nelson MT, Joksovic PM, Perez-Reyes E and Todorovic SM (2005) The endogenous redox agent L-cysteine induces T-type Ca^{2+} channel-dependent sensitization of a novel subpopulation of rat peripheral nociceptors. *J Neurosci* **25**: 8766-75.

Nelson MT, Woo J, Kang H-W, Barrett PQ, Vitko J, Perez-Reyes E, Lee J-H, Shin H-S and Todorovic SM (2007) Reducing agents sensitize C-type nociceptors by relieving high-affinity zinc inhibition of T-type calcium channels. *J Neurosci* **27**: 8250–8260.

Orestes P, Bojadzic D, Lee J, Leach E, Salajegheh R, Digruccio MR, Nelson MT and Todorovic SM (2011) Free radical signaling underlies inhibition of CaV3.2 T-type calcium channels by nitrous oxide in the pain pathway. *J Physiol* **589.1**: 135-148.

Pathirathna S, Brimelow BC, Jagodic MM, Kathiresan K, Jiang X, Zorumski CF, Mennerick S, Covey DF, Todorovic SM and Jevtovic-Todorovic V (2005) New evidence that both T-type Ca^{2+} channels and $GABA_A$ channels are responsible for the potent peripheral analgesic effects of 5α-reduced neuroactive steroids. *Pain* **114**:429-443.

Pathirathna S, Todorovic SM, Covey DF and Jevtovic-Todorovic V (2005) 5α-reduced neuroactive steroids alleviate thermal and mechanical hyperalgesia in rats with neuropathic pain. *Pain* **117**: 326-39.

Perez-Reyes E, Cribbs LL, Daud A, Lacerda AE, Barclay J, Wiliamson MP, Fox M, Rees M and Lee J (1998) Molecular characterization of a neuronal low-voltage-activated T-type calcium channel. *Nature* **391**: 896-900.

Perez-Reyes E (2003) Molecular physiology of low-voltage-activated T-type calcium channels. *Physiol Rev* **83**:117-161.

Randall A and Tsien RW (1997) Contrasting biophysical and pharmacological properties of T-type and R-type calcium channels. *Neuropharmacol* **36**:879-893.

Rogawski MA and Loscher W (2004) The neurobiology of antiepileptic drugs for the treatment of nonepileptic conditions. *Nat Med* **10(7)**:685-92.

Shipe WD, Barrow JC, Yang Z-Q et al (2008) Design synthesis and evaluation of a novel 4-aminomethyl-4-fluoropiperidine as a T-type Ca^{2+} channel antagonist. *J Med Chem* **51(13)**:3692-3695.

Sidach SS and Mintz IM (2002) Kurtoxin, a gating modifier of neuronal high- and low-threshold ca channels. *J Neurosci* **22(6)**:2023-34.

Snutch TP and David LS (2005) T-type calcium channels: an emerging therapeutic target for the treatment of pain. *Drug Development Research* 67 (4): 404 - 415.

Tang CM, Presser F and Morad M (1988) Amiloride selectively blocks the low threshold (T)-type calcium channel. *Science Wash DC* **240**:213-215.

Todorovic SM, Jevtovic-Todorovic V, Meyenburg A, Mennerick S, Perez-Reyes E, Romano C, Olney JW and Zorumski CF (2001) Redox modulation of T-type calcium channels in rat peripheral nociceptors. *Neuron* **31**: 75-85.

Todorovic SM and Lingle CJ (1998) Pharmacological properties of T-type Ca^{2+} current in adult rat sensory neurons: effects of anticonvulsant and anesthetic agents. *J Neurophysiol* **79**: 240-52.

Todorovic SM, Meyenburg A and Jevtovic-Todorovic V (2002) Mechanical and thermal antinociception in rats following systemic administration of mibefradil, a T-type calcium channel blocker. *Brain Research* **951**: 336-340.

Todorovic SM, Meyenburg A and Jevtovic-Todorovic V (2004) Redox modulation of peripheral T-type Ca^{2+} channels in vivo: alteration of nerve injury-induced thermal hyperalgesia. *Pain* **109**: 328-339.

Todorovic SM, Prakriya M, Nakashima YM, Nilsson KR, Han M, Zorumski CF, Covey DF and Lingle CJ (1998) Enantioselective blockade of T-type Ca2+ current in adult rat sensory neurons by a steroid that lacks gamma-aminobutyric acid-modulatory activity. *Mol Pharmacol* **54**:918-27.

Todorovic SM, Rastogi AJ and Jevtovic-Todorovic V (2003) Potent analgesic effects of anticonvulsants on peripheral thermal nociception in rats. *Br J Pharmacol* **140**:255-260.

Todorovic SM, Pathirathna S, Brimelow BC, Jagodic MM, Ko SH, Jiang X, Nilsson KR, Zorumski CF, Covey DF and Jevtovic-Todorovic V (2004) 5β-reduced neuroactive steroids are novel voltage-dependent blockers of T-type Ca2+ channels in rat sensory neurons in vitro and potent peripheral analgesics in vivo. *Mol Pharmacol* **66**: 1223-1235.

White G, Lovinger DM and Weight FF (1989) Transient low-threshold Ca^{2+} current triggers burst firing through an afterdepolarizing potential in an adult mammalian neuron. *PNAS USA* **86**: 6802-6806.

Woolf CJ (2004) Dissecting out mechanisms responsible for peripheral neuropathic pain: implications for diagnosis and therapy. *Life Sci* **74**: 2605-2610.

Zamponi GW, Bourinet E and Snutch TP (1996) Nickel block of a family of neuronal calcium channels: subtype- and subunit-dependent action at multiple sites. *J Membr Bio* **151**: 77–90.

Molecular Pharmacology Fast Forward. Published on August 5, 2011 as DOI: 10.1124/mol.111.073205
This article has not been copyedited and formatted. The final version may differ from this version.

FOOTNOTES

a) Our research is supported by Dr. Harold Carron's endowment, National Institute for Health R21 grant [DA029342], American Diabetes Association Basic Research grant [7-09-BS-190], funds from the Department of Anesthesiology at the University of Virginia, funds from InJe University and generous gift from Mr. Joseph C. Palumbo and Mrs. Sandra C. Palumbo. We thank Mr. Damir Bojadzic for technical assistance and Dr. Toni Schneider for providing stable cell lines expressing $Ca_V2.3\beta3$ subunits. We thank Dr. Victor N. Uebele and Dr. John J. Renger from the Department of Neurology, MERCK Res. Lab., West Point, PA for providing the TTA-P2 compound, support of experimental design and review of the manuscript.

b) Reprint requests to Slobodan M. Todorovic, Department of Anesthesiology, University of Virginia Health System, 1 Hospital Drive, Mail Box 800710, Charlottesville, VA 22908-0710

Molecular Pharmacology Fast Forward. Published on August 5, 2011 as DOI: 10.1124/mol.111.073205
This article has not been copyedited and formatted. The final version may differ from this version.

FIGURE LEGENDS

Figure 1. The structure of TTA-P2 compound evaluated in this study.

Figure 2. TTA-P2 selectively inhibits T-currents in acutely dissociated adult rat sensory neurons.

A. Traces of T-current in a representative DRG cell before and after (black traces), as well as during (gray trace) bath application of 1 μM TTA-P2, which reversibly inhibited most of the peak inward current. Currents were evoked from holding potential (V_h) of -90 mV and stepping to test potential (V_t) of -30 mV. Bars indicate calibration.

B. Temporal record from the same cell presented in panel A of this figure. Gray bar indicates duration of TTA-P2 application.

C. Traces of HVA current from another DRG cell before (black trace) and during (gray trace) the bath application of 10 μM TTA-P2. TTA-P2 inhibited less than 10% of peak current. Currents were evoked from V_h of -50 mV and stepping to V_t of -10 mV. Bars indicate calibration.

D. Traces of recombinant $Ca_V2.3$ current from a representative HEK293 cell before (black trace) and during (gray trace) the bath application of 10 μM TTA-P2, which inhibited about 20% of the peak current. Currents were evoked from V_h of -80 mV and stepping to V_t of -20 mV. Bars indicate calibration.

E. Traces of total sodium current (I_{Na+}) from a representative DRG cell are shown on the left. Traces of TTX-resistant sodium current ($I_{Na+\ TTXR}$) from another DRG cell are presented on the right. Note that there is little difference between baseline current (black traces) and during the bath application (gray traces) of 1 μM TTA-P2. Currents are evoked from V_h of -90 mV and stepping to V_t of -20 mV. Bars indicate calibration.

Molecular Pharmacology Fast Forward. Published on August 5, 2011 as DOI: 10.1124/mol.111.073205
This article has not been copyedited and formatted. The final version may differ from this version.

Figure 3. TTA-P2 inhibits T-currents in DRG cells more potently than it does HVA currents in DRG cells and recombinant $Ca_V2.3$ currents in HEK 293 cells.

The graphs illustrate concentration-response relationships for TTA-P2 inhibition of T-currents in rat DRG cells (filled circles), HVA currents in DRG cells (filled squares), and recombinant $Ca_V2.3$ currents in HEK293 cells (open triangles) (n = 4-15 cells per data point). Solid line is the best fit (equation # 1, Methods) for T-current inhibition: IC_{50} of 0.11 ± 0.01 μM, slope coefficient 0.8 ± 0.1, and maximal inhibition of 90 ± 3% of the peak current; for HVA current inhibition: IC_{50} of 165 ± 35 μM, slope coefficient 1.3 ± 0.5,, and maximal inhibition constrained to 100%; for $Ca_V2.3$ current inhibition: IC_{50} of 35 ± 9 μM, slope coefficient 0.9 ± 0.3, and maximal inhibition constrained to 100%.

Figure 4. The effects of TTA-P2 on kinetic properties of T-currents in rat DRG cells.

A. Traces represent families of averaged T-currents evoked in the same DRG cells (n=5) in control conditions (top panel) and during application of 100 nM TTA-P2 (lower panel) by voltage steps from -90 mV (V_h) to V_t from -60 through -20 mV in 10-mV increments. Bars indicate calibration. Inset at the top of this panel represents voltage-clamp protocol used to elicit currents.

B. Average I-V curves are shown from the same DRG cells shown in panel A before (open symbols) and during (filled symbols) bath application of 100 nM TTA-P2 using voltage steps in 5-mV increments. Note that TTA-P2 depressed the amplitude of T-current similarly at most test potentials.

C, D. We measured time-dependent activation (10%-90% rise time, panel D) and inactivation τ (single exponential fit of decaying portion of the current waveforms using equation # 4, panel C) from I-V curves in DRG cells shown in panel B over the range of

Molecular Pharmacology Fast Forward. Published on August 5, 2011 as DOI: 10.1124/mol.111.073205
This article has not been copyedited and formatted. The final version may differ from this version.

test potentials from -45 mV to -20 mV. There are few differences between the control (open symbols) and TTA-P2 groups (filled symbols) with the exception of the 10%-90% rise time at -40 mV (panel D). Symbol * indicates $p < 0.05$

E. Data points for channel conductance (G) are calculated from the graph presented in panel B by dividing current amplitudes with the driving force for ion permeation. Estimated reversal potential was taken to be 60 mV. Solid lines are fitted using equation # 2 (Methods), giving half-maximal conductance (V_{50}), which occurred at -43.2 ± 0.6 mV with a slope *k* of 4.5 ± 0.6 mV in control conditions (open symbols). Similarly, V_{50} was -43.6 ± 0.3 mV with a *k* of 3.5 ± 1.0 mV during TTA-P2 application (filled symbols).

F. Deactivating tail currents in controls (open symbols) and during application (filled symbols) of 100 nM TTA-P2 were fit with a single exponential function. The resulting tau values are plotted (n = 5 cells). Points that are statistically significant are marked with an asterisk ($p < 0.05$). Inset represents voltage-clamp protocol.

Vertical lines in panels B, C, D, and F represent SEM of multiple determinations.

Figure 5. Effects of TTA-P2 on steady-state-inactivation and recovery from inactivation of T-currents in rat DRG cells.

A. Current availability curves at different conditioning potentials before and during application of 100 nM TTA-P2 to the same cells are presented in the top panel.

B. The same data are normalized for clarity of presentation in the lower panel of this figure (n = 4 cells). Open symbols represent the control conditions; filled symbols represent the conditions during bath application of TTA-P2. Solid black lines are fitted using equation # 3 (Methods), giving half-maximal availability (V_{50}), which occurred at -67.5 ± 0.3 mV with a slope *k* of 6.7 ± 0.3 mV in control conditions. In contrast, fitted V_{50} was -90 ± 1 mV with a *k* of 8.7 ± 1.0 mV in the conditions when TTA-P2 was applied.

Molecular Pharmacology Fast Forward. Published on August 5, 2011 as DOI: 10.1124/mol.111.073205
This article has not been copyedited and formatted. The final version may differ from this version.

Vertical lines represent SEM of multiple determinations. Inset represents voltage-clamp protocol.

C. TTA-P2 impairs recovery from inactivation in DRG cells. Symbols on the graph indicate averaged data from multiple cells (n = 5) and solid lines were fitted with a double exponential equation (equation # 5, Methods): yielding in pre-drug control: τ1, 2388 ± 300 msec, τ2, 155 ± 15 msec; TTA-P2: τ1, 1045 ± 181 msec, τ2, 43 ± 15 msec; Note that in the presence of TTA-P2 currents recovered (P2/P1) only to about 60% of control current (*, $p<0.05$). If the fitting curve in the presence of TTA-P2 was constrained to 100 % recovery, we obtained the following recovery τs: τ1, 16130 ± 4316 msec, τ2, 165 ± 50 msec (data not shown). Inset represents voltage-clamp protocol for our double-pulse protocol.

Figure 6: TTA-P2 has antinocicpetive properties in the formalin pain model and has no effect on sensorimotor tests in mice.

A. Adult mice experience significant analgesia after i.p. injections of TTA-P2 at 5 mg/kg (open bars, n = 8) or 7.5 mg/kg (gray bars, n = 14) as compared to experiments with vehicle (control, black bars, n = 15). Vertical bars indicate SEM; * indicates a significance of $p < 0.01$ by Student t-test.

B. Panels show histograms of average time in sec in different sensorimotor tests using an inclined plane (panel A), platform (panel B), and ledge (panel C) for mice injected with 5 mg/kg of TTA-P2 (white bars) or 7.5 mg/kg of TTA-P2 (gray bars). Baseline measurements were taken 2 days before (controls, black bars). Note that black bars indicate controls with two different groups of animals injected subsequently with either 5 mg/kg or 7.5 mg/kg of TTA-P2. Vertical bars indicate SEM of multiple determinations. At either dose, TTA-P2 had no significant effect on either test, since $p > 0.05$ in

Molecular Pharmacology Fast Forward. Published on August 5, 2011 as DOI: 10.1124/mol.111.073205
This article has not been copyedited and formatted. The final version may differ from this version.

comparisons of time points between controls and after injections of TTA-P2 (n = 6 mice in each group).

Figure 7. TTA-P2 effectively reverses hyperalgesia in diabetic STZ-treated rats but does not change baseline nociceptive thresholds in healthy rats.

The upper panel shows that baseline (B) PWLs in right paws (open bars) and left paws (dark bars) remain stable 1 hr after i.p. injections of TTA-P2 at 5, 7.5, or 10 mg/kg. The middle panel shows the dose-dependent antihyperalgesic effect of TTA-P2, which, at 10 mg/kg i.p., completely reversed thermal hyperalgesia in STZ-treated diabetic rats. Note that AS treatment (lower panel) also completely reversed diabetic hyperalgesia, as indicated by the apparent normalization of PWLs, and that subsequent applications of TTA-P2 at different doses did not change PWLs.

Vertical bars on all panels indicate SEM of multiple experiments (n = 4-8 per group).

* indicates $p < 0 .05$ baseline (B) versus treatment at different doses of TTA-P2.

$^{+}$ indicates $p < 0.05$ for treatment with TTA-P2 versus new baseline in diabetic rats (STZ).

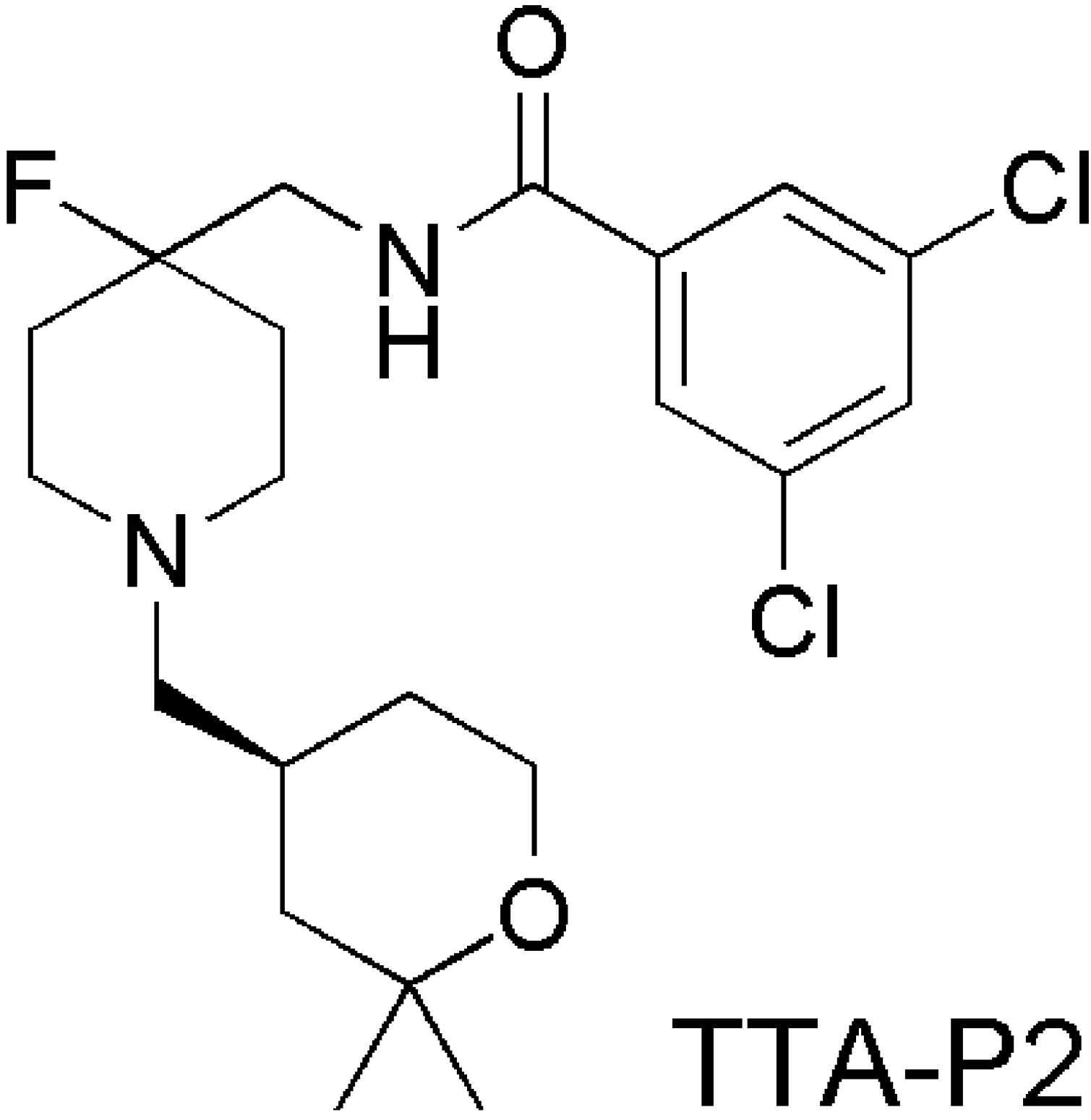

TTA-P2

Figure 2

A

DRG I_T

1 μM TTA-P2

50 pA

wash

25 ms

control

B

DRG I_T

1 μM TTA-P2

Peak I_T (pA)

-200
-160
-120
-80
-40
0

0
200
400
600

Time Elapsed (sec)

C

DRG I_{HVA}

200 pA

50 ms

10 μM TTA-P2

control

D

$I_{CaV2.3}$

10 μM TTA-P2

200 pA

50 ms

control

E

DRG I_{Na+}

control

1 μM TTA-P2

500 pA

2 ms

DRG $I_{Na+\ TTXR}$

200 pA

10 ms

Figure 3

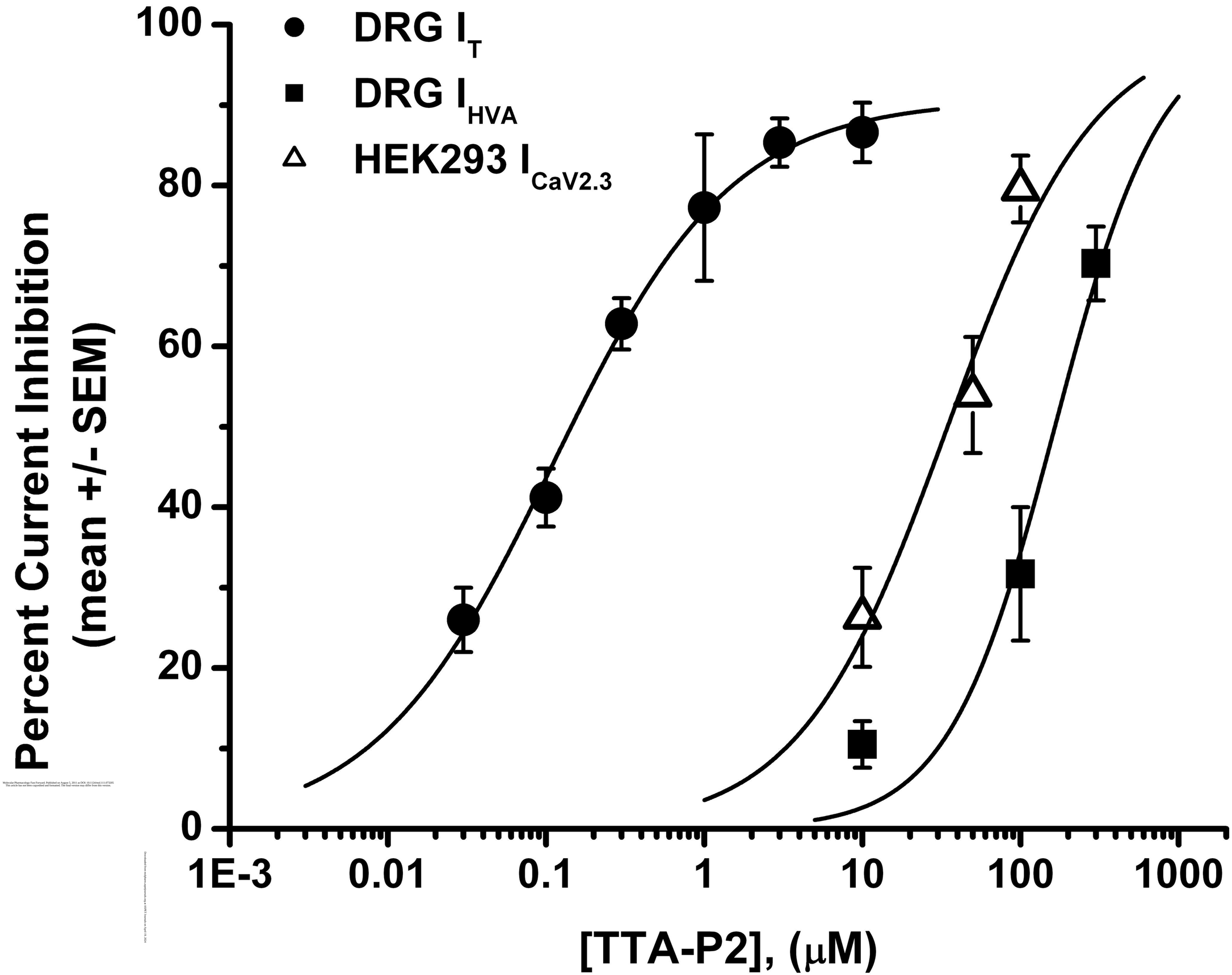

Figure 4

A

V_h -90 mV

V_t -60 mV through -20 mV

200 pA

25 ms

Control

TTA-P2

B

Percent Peak T-current

0

40

80

120

Control

TTA-P2

-60

-40

-20

Test Potential (mV)

C

Inactivation Tau (msec)

100

80

60

40

20

0

Control

TTA-P2

-50

-40

-30

-20

D

Test Potential (mV)

10-90% Rise Time (msec)

40

30

20

10

0

*

Control

TTA-P2

-50

-40

-30

-20

E

Test Potential (mV)

G/Gmax

120

80

40

0

Control

TTA-P2

-60

-40

-20

Test Potential (mV)

F

Test Potential (mV)

-30 mV

-60 mV

-90 mV

-160 mV

Deactivation Tau (msec)

4

3

2

1

0

*

Control

TTA-P2

-160

-120

-80

-40

Potential (mV)

Figure 5

A

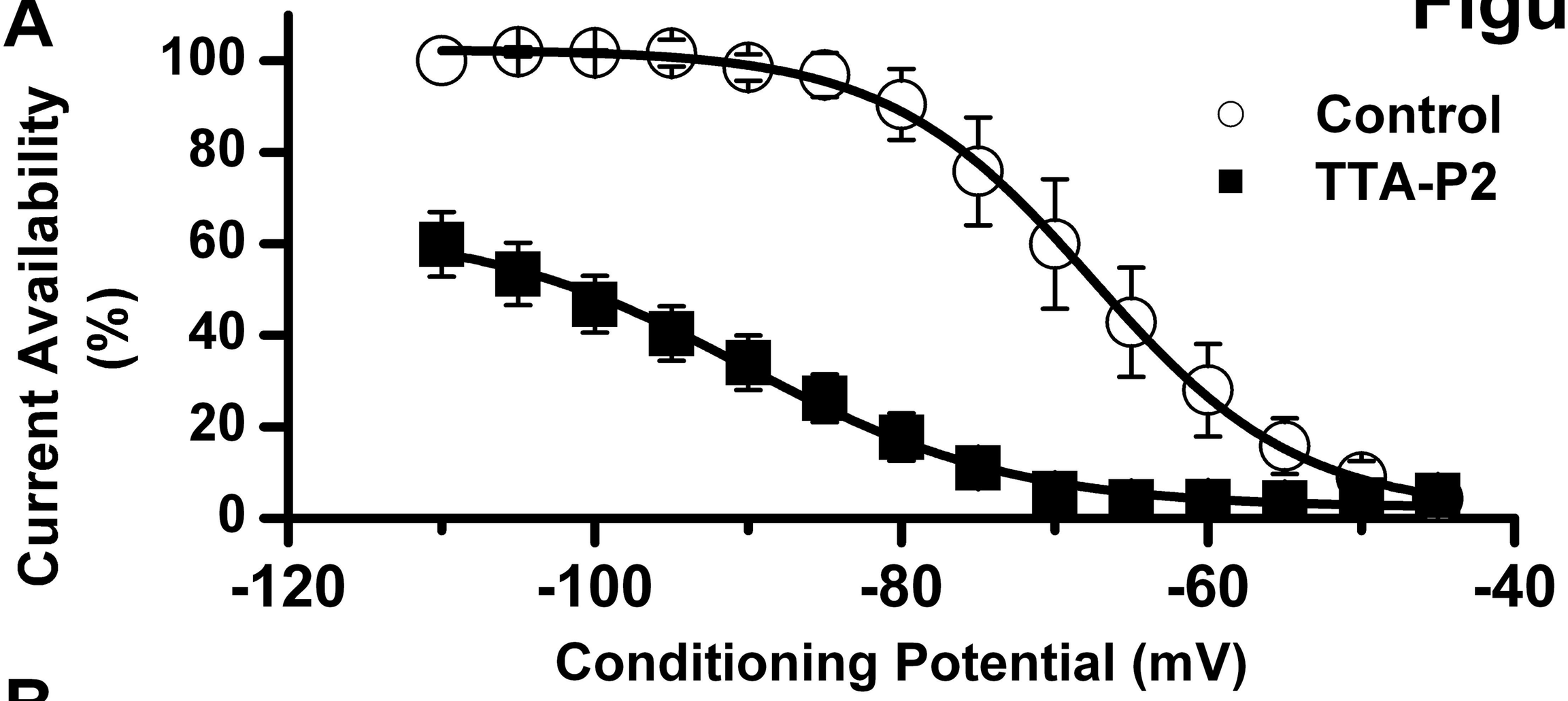

B

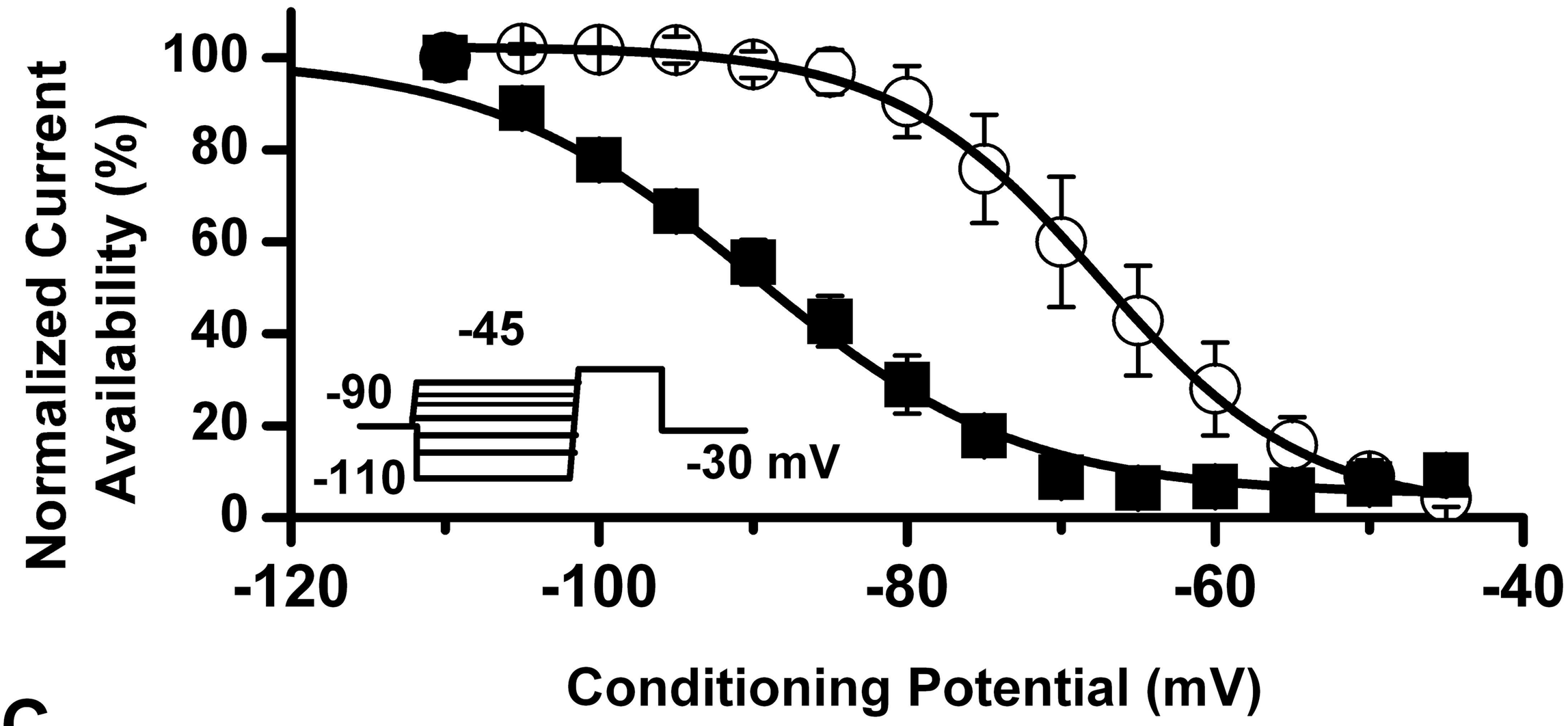

C

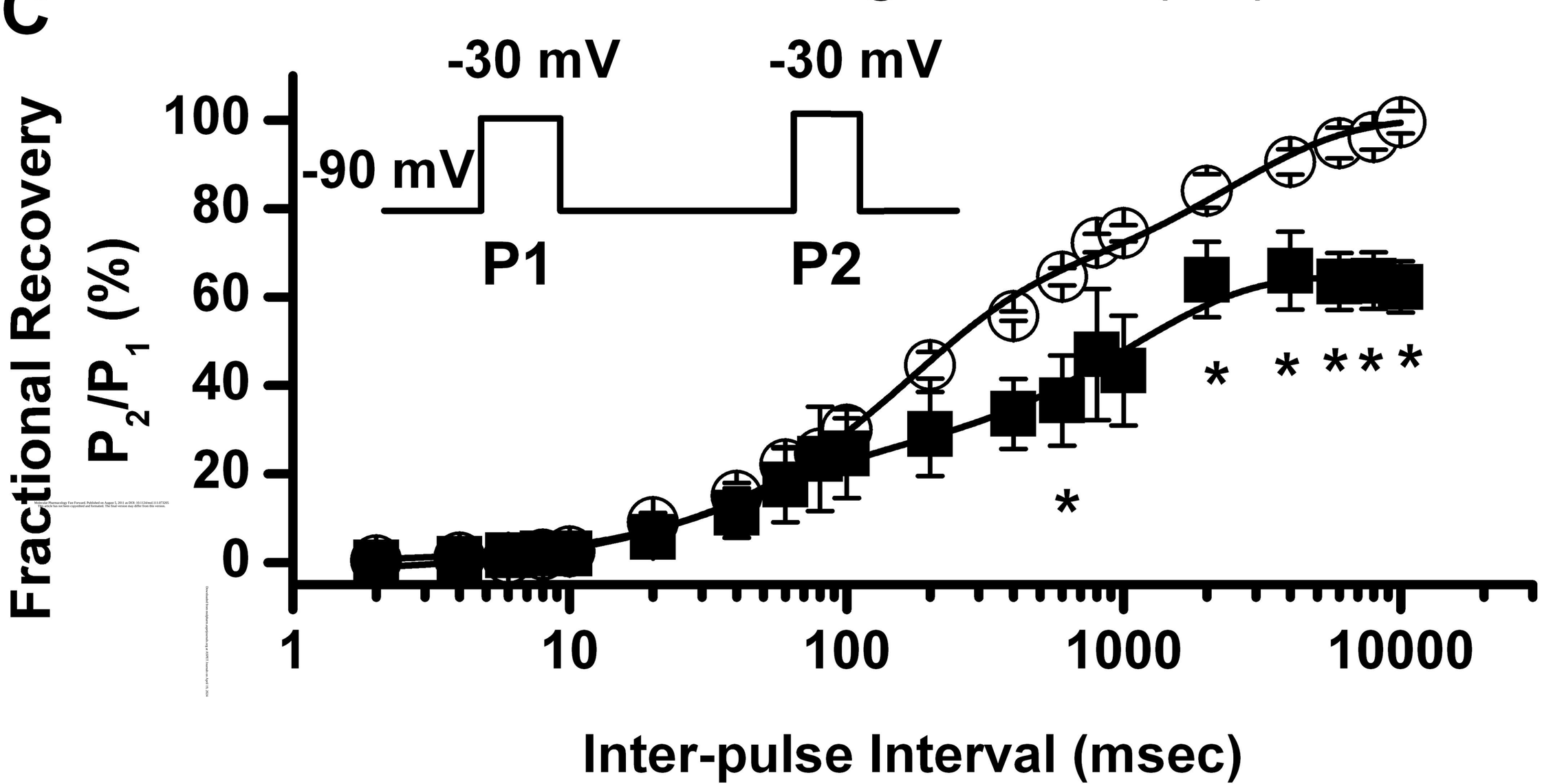

Figure 6

A

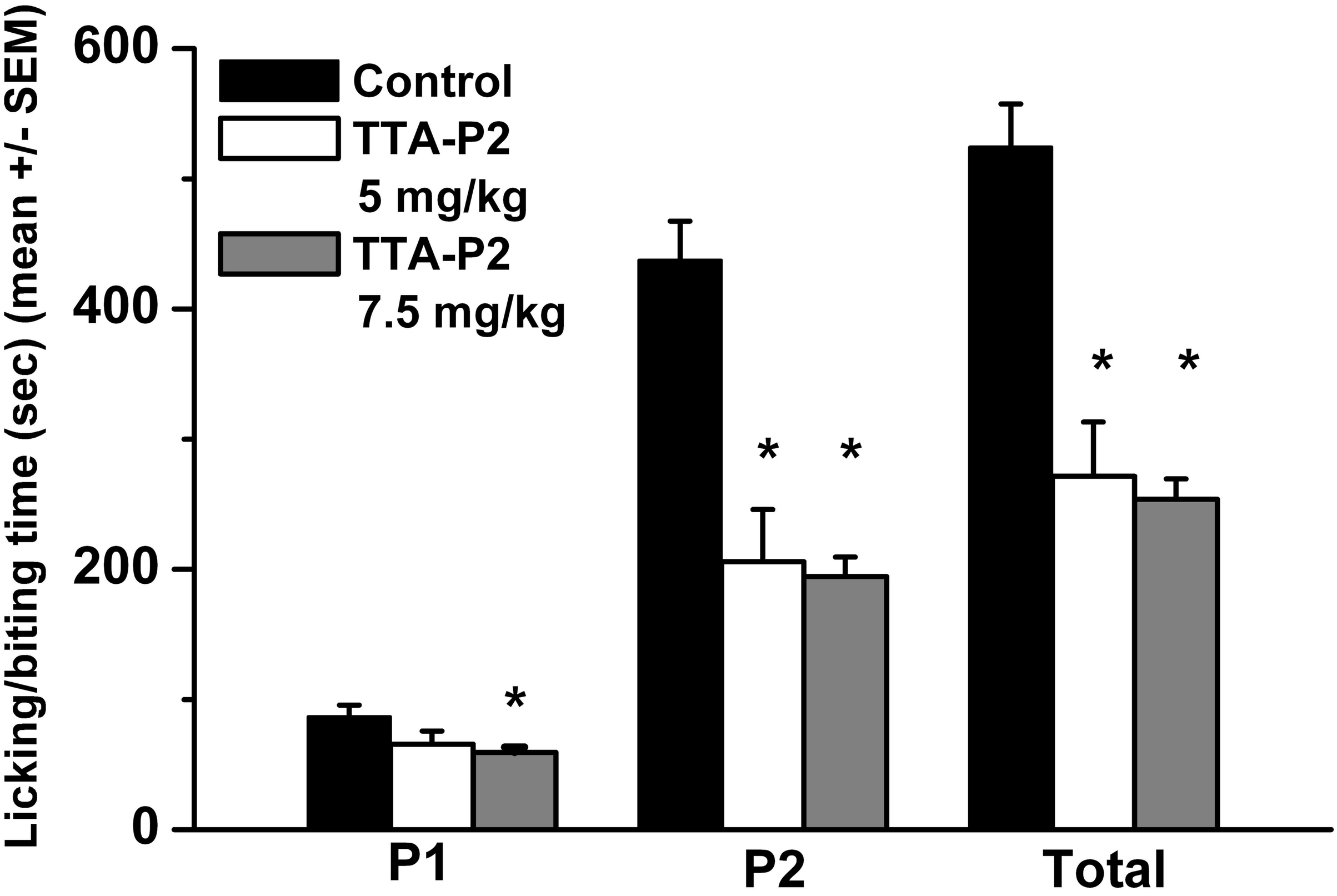

B

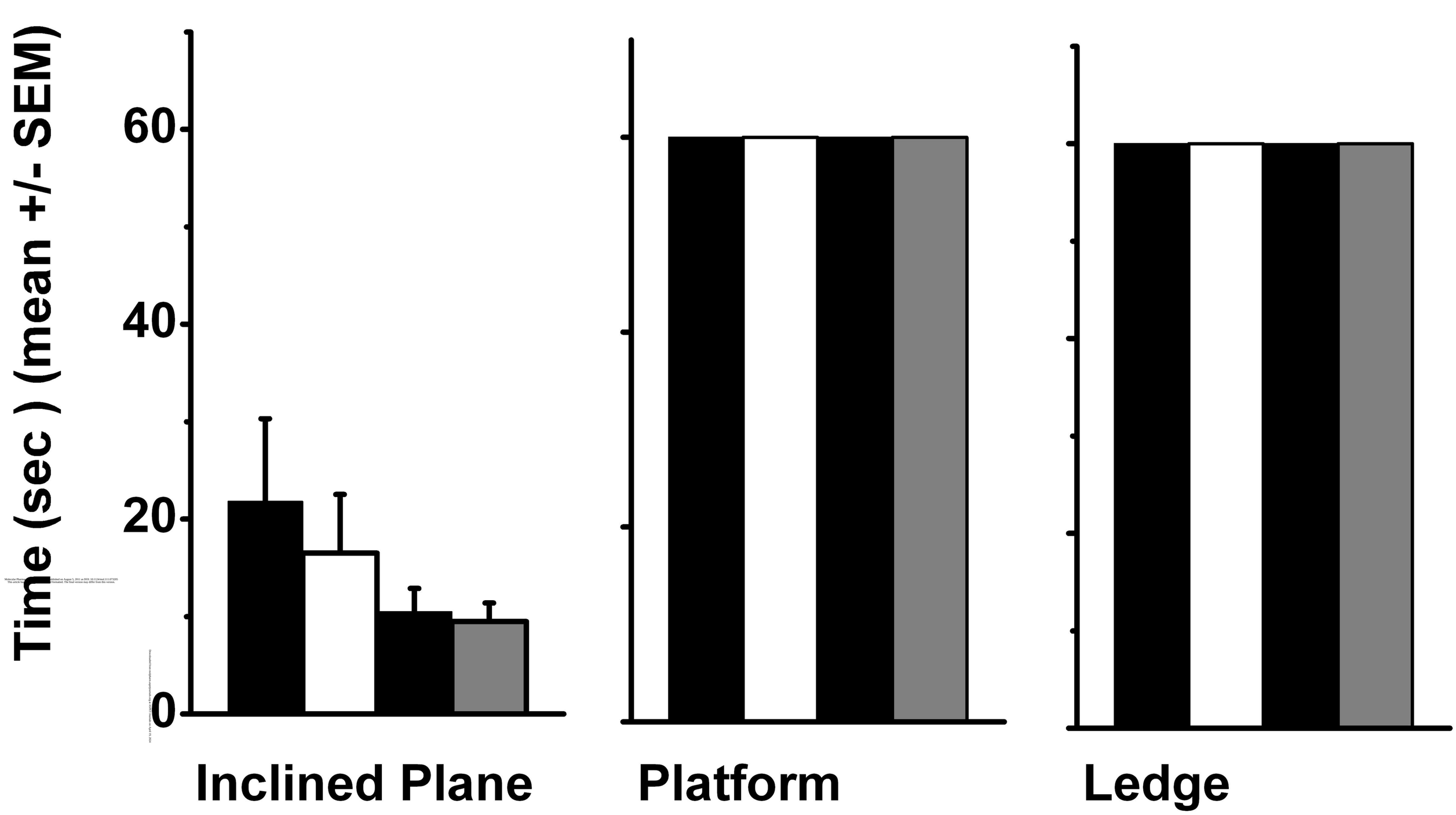

Figure 7

Healthy

Right Paw
Left Paw

12.5
10.0
7.5
5.0

B
TTA-P2 5
TTA-P2 7.5
TTA-P2 10mg/kg

Diabetic

PWL (sec) (mean +/- SE

12.5
10.0
7.5
5.0

*
*
*
+

B
STZ
TTA-P2 5
TTA-P2 7.5
TTA-P2 10mg/kg

Diabetic

12.5
10.0
7.5
5.0

*
+
+
+
+

B
STZ
AS
TTA-P2 5
TTA-P2 7.5
TTA-P2 10mg/kg